Article

Anatomy, Age and Origin of an Intramontane Top Basin Surface (Sorbas Basin, Betic Cordillera, SE Spain)

Martin Stokes [1,*] **, Anne E. Mather** [1]**, Ángel Rodés** [2]**, Samantha H. Kearsey** [1,†] **and Shaun Lewin** [1]

1   School of Geography, Earth and Environmental Sciences, University of Plymouth, Drake Circus, Plymouth, Devon PL4 8AA, UK; amather@plymouth.ac.uk (A.E.M.); samantha.kearsey1@gmail.com (S.H.K.); shaun.lewin@plymouth.ac.uk (S.L.)
2   Natural Environment Research Council (NERC) Cosmogenic Isotope Analysis Facility, Scottish Universities Environmental Research Centre, Rankine Avenue, Scottish Enterprise Technology Park, East Kilbride G75 0QF, UK; Angel.Rodes@glasgow.ac.uk
*   Correspondence: mstokes@plymouth.ac.uk; Tel.: +44-1752-584772
†   Née Samantha H. Ilott.

Academic Editors: Xianyan Wang, Jef Vandenberghe and David Bridgland

Abstract: Collisional mountain belts commonly develop intramontane basins from mechanical and isostatic subsidence during orogenic development. These frequently display a relict top surface, evidencing a change interval from basin infilling to erosion often via capture or overspill. Such surfaces provide markers that inform on orogenic growth patterns via climate and base level interplay. Here, we describe the top surface from the Sorbas Basin, a key intramontane basin within the Betic Cordillera (SE Spain). The surface is fragmentary comprising high elevation hilltops and discontinuous ridges developed onto the variably deformed final basin infill outcrop (Gochar Formation). We reconstruct surface configuration using DEM interpolation and apply ^{10}Be/^{26}Al cosmonuclides to assess surface formation timing. The surface is a degraded Early Pleistocene erosional pediment developed via autogenic switching of alluvial fan streams under stable dryland climate and base level conditions. Base-level lowering since the Middle Pleistocene focused headwards incision up interfan drainages, culminating in fan head capture and fan morphological preservation within the abandoned surface. Post abandonment erosion has lowered the basin surface by 31 m (average) and removed ~5.95 km^3 of fill. Regional basin comparisons reveal a phase of Early Pleistocene surface formation, marking landscape stability following the most recent Pliocene-Early Pleistocene mountain building. Post-surface erosion rate quantification is low and in accordance with ^{10}Be denudation rates typical of the low uplift Betic Cordillera.

Keywords: intramontane basin; pediment; glacis; alluvial fan; river terrace; DEM; interpolation; cosmonuclide; base level

1. Introduction

Intramontane basins are areas of fault and fold-related subsidence that develop within an evolving collisional mountain belt [1]. The tectonically dynamic nature of such settings means that intramontane basins can cyclically form, fill and erode over geological timescales [2,3]. The basins can be internally drained, dominated by alluvial fan and lacustrine settings, but can then switch to externally drained systems via lake overspill or river capture processes [4,5]. Studies of intramontane basins are either (1) geological, focusing on the sedimentary infill record for stratigraphic, palaeoenvironmental and

tectonic purposes [6] or (2) geomorphological, using inset river-fan-lake terrace levels to reconstruct the basin incisional history linked to tectonic-climatic-capture-related changes in sediment supply and base level [7]. A key, but often overlooked stratigraphic unit is the surface that caps the final stage of intramontane basin infill. This surface can be (1) depositional, with a morphology reflecting the final depositional environment(s) (alluvial fan/lake) or (2) erosional, formed by regional subaerial processes. Such 'epigene' land surfaces (sensu Watchman and Twidale [8]) are scientifically important because they mark the point at which the basin has switched from erosion to deposition [9]. Furthermore, they can act as a regional marker, providing insight into patterns and drivers of the onset and subsequent basin incision [10] or as a marker for surface deformation assessments [11]. However, these surfaces can be problematic to study due to poor preservation, post depositional modification and dating challenges meaning the surfaces often only attract peripheral attention as the respective end or start context points of geological and geomorphological research. For example, surface remnants are often highly fragmentary and can be degraded by erosion or deformation causing across basin or between basin correlation problems [12,13]. Once abandoned, the surface can become modified due to cementation by pedogenic or groundwater processes [14]. Surface dating can be a significant challenge due to technique limitations or material suitability issues collectively related to surface composition, degradation because of surface antiquity (i.e., surface is beyond the technique age range limit) and post depositional degradation and modification also linked to antiquity [15,16]. To explore and overcome some of these challenges and to highlight the importance of intramontane top basin surfaces for understanding sedimentary basin evolution and longer-term Quaternary landscape development we examine the Sorbas Basin in SE Spain (Figure 1). The Sorbas Basin is a medium sized (30 × 20 km) Neogene sedimentary basin that has developed as part of the ongoing fault and fold related uplift of the Betic Cordillera, a major Alpine mountain range, formed because of the ongoing Africa-Europe collision [2]. The basin fill is dominated by marine Miocene sedimentation [17,18], with continental sedimentation forming the final stages of basin infill (Gochar Formation [19,20]).
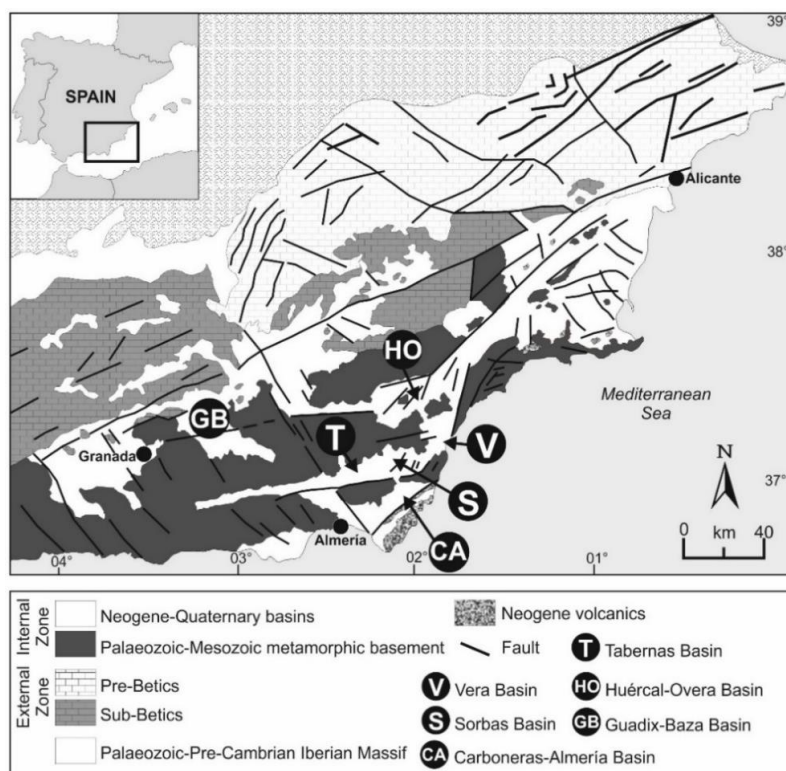

Figure 1. Tectonic zonation of the Betic Cordillera and key intramontane basins referred to within the text (modified from [21–23]).

A surface is developed onto the final stage of basin fill, commonly referred to as the "Gochar Surface" by studies examining long-term drainage evolution [10,24]. The purpose of this paper is to: (1) describe the relict morphology of the basin surface, (2) to digitally reconstruct the surface using interpolation of surface remnants, (3) to provide age estimates for surface development using cosmonuclide dating; (4) to use the interpolated and dated surface to quantify spatial and temporal patterns of basin erosion and (5) to consider the development of the surface as a Quaternary landscape feature in the context of the ongoing cyclic development of an intramontane basin.

2. Geological and Geomorphological Background

The Sorbas Basin (Figures 1 and 2) is one of a series of Neogene intramontane sedimentary basins within the Betic Cordillera [2]. It is defined to the north and south by mountain ranges of metamorphic basement (Figure 2) that are organized into km-scale regional antiformal fold structures formed in consequence of Miocene-Recent collision-related tectonic denudation [25,26]. The Sierra de los Filabres to north peaks at 1304 m (Ermita de la Virgen de la Cabeza) and comprises an embayed non-faulted mountain front with a relief of up to 700 m. To the south, the Sierra Alhamilla is characterised by a linear faulted mountain front [27], peaking at 1004 m (Cerrón de Lucainena) and with a relief of ~400 m. The intervening basin is infilled with a sequence of Miocene to Quaternary marine and continental sediments that are folded into an open E-W orientated syncline structure (Figure 2). The basin narrows to the west and east, joining the adjacent Tabernas and Vera Basins, delimited by poorly defined topographic highs developed into the sedimentary infill.
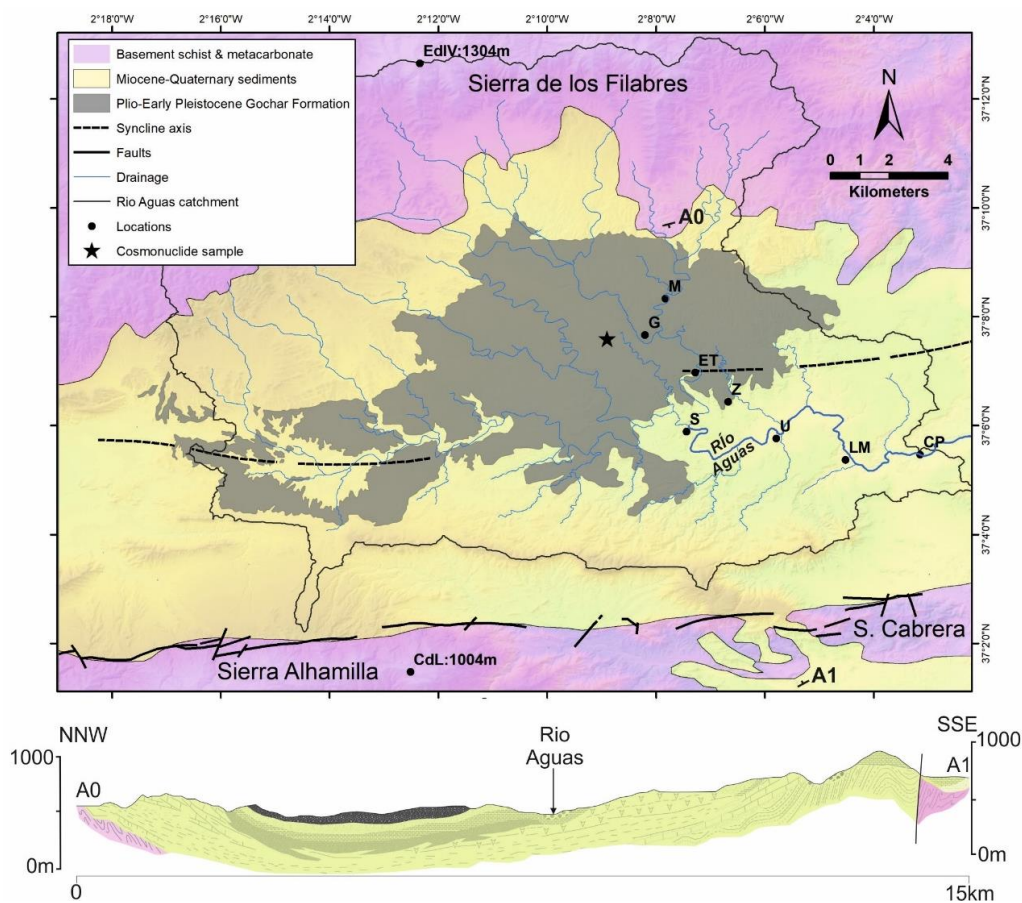

Figure 2. Simplified Sorbas Basin geology map and cross section (modified from [28,29]). EdlV: Ermita de la Virgen; M: Moras; G: Gochar; ET: El Tieso; S: Sorbas; Z: Zorreras; U: Urra; LM: Los Molinos; CP: capture point; CdL: Cerron de Lucainena; A0-A1: line of section.

Miocene marine sediments dominate the Sorbas Basin sedimentary infill (Figure 3), becoming progressively continental during the late Miocene represented by coastal plain sediments (Zorreras Member) and basin margin alluvial fan sequences (Moras Member) [19].
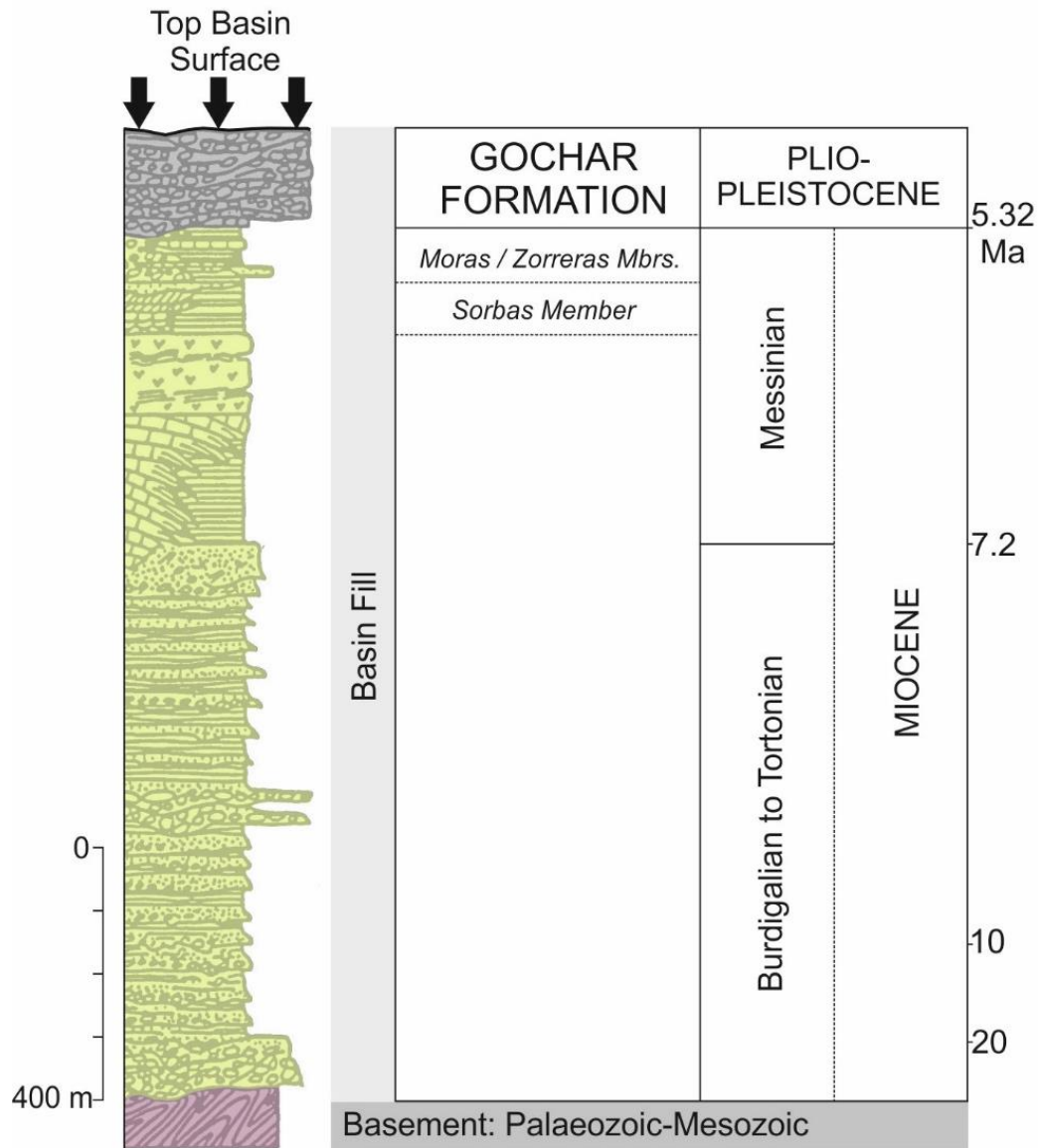

Figure 3. Simplified composite graphic log of the Sorbas Basin sedimentary infill (modified from [19]) illustrating key stratigraphic units referred to within the text and other figures.

The end Zorreras Member is stratigraphically important, being constrained to the Mio-Pliocene boundary from magnetostratigraphic and biostratigraphic studies [30,31]. Furthermore, the Zorreras Member lacustrine-marine bands have been used as marker horizons to demonstrate spatially variable Plio-Quaternary uplift patterns, ranging from 0.08 to 0.16 mm^{a-1} from the basin centre to the southern margin [19].

The overlying Gochar Formation (Figure 3) represents the final infilling stage of the Sorbas Basin, forming an outcrop of ~80 km^2 (Figure 2). It comprises a 40–200 m thick conglomerate and sandstone sequence deposited by alluvial fans and braided rivers [19,20,32] with spatially and temporally variable degrees of syn- and post-depositional deformation [19]. The fan and river systems are organised into four distinct drainage systems based on variations in sedimentology, provenance and palaeocurrent

directions [19,20,32]. These drainage systems are important for the morphological development of the top basin surface, providing a relict topography onto which surface erosion occurred. The timing of the Gochar Formation is unclear as it lacks any direct age control, with a broad assignment to the Plio-Quaternary based upon stratigraphic bracketing with the Miocene basin fill (Zorreras Member) and Pleistocene river terraces.

Post Gochar Formation the Sorbas Basin has undergone incision, reflected in the development of an inset Pleistocene river terrace sequence [24] with coeval landslide, karst and badland development [33,34]. The river terraces (Figure 4) are configured into up to 5 inset levels (labelled A to E, where A: highest and oldest, and E: lowest and youngest), comprising up to 20 m thick aggradations of undeformed conglomerate capped by varying degrees of calcrete and soil reddening dependent on relative age [35].
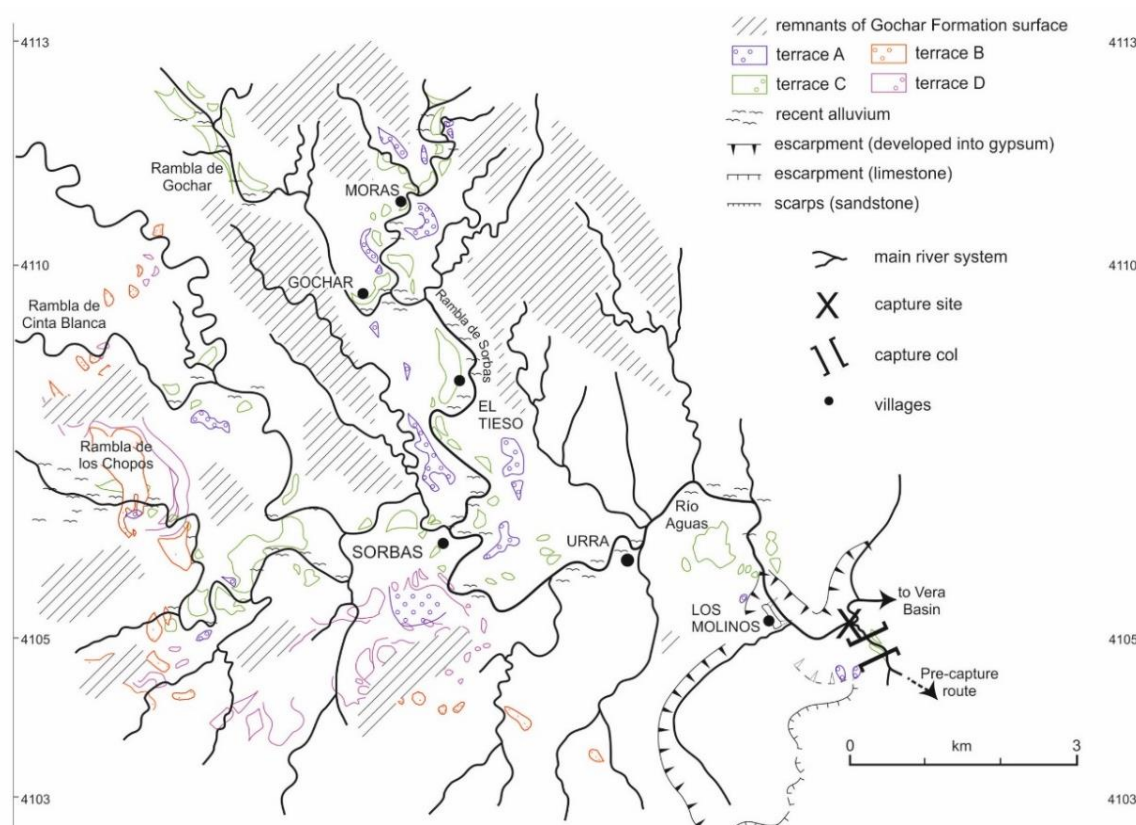

Figure 4. Sorbas Basin Middle-Late Pleistocene river terrace map (modified from [10]). See Figure 2 for catchment-scale overview.

Terrace level A can be inset by up to 20 m into the Gochar Formation sediments (Figure 5), with the entire terrace sequence recording between 40 m to 160 m of incision between upstream (Moras) and downstream (Los Molinos) regions [10]. These incision patterns are linked to spatially variable base-level lowering driven by combinations of regional uplift variability and river capture [12,24]. Terrace ages span the Middle-Late Pleistocene based on a range of radiometric and luminescence techniques [24,36–38]. The terraces are developed along the valleys of the trunk drainage (Río Aguas) and its major tributaries (Ramblas de Gochar, Moras, Cinta Blanca, los Chopos, etc.) (Figure 4). Terraces have formed within a catchment area of ~285 km^2 upstream of the Aguas-Feos capture point (Figures 2, 4 and 5), the site of a major basin-scale capture that occurred ~100 ka, beheading and re-routing the former southwards flowing drainage (Rambla de los Feos) to the east into the Vera Basin [24].
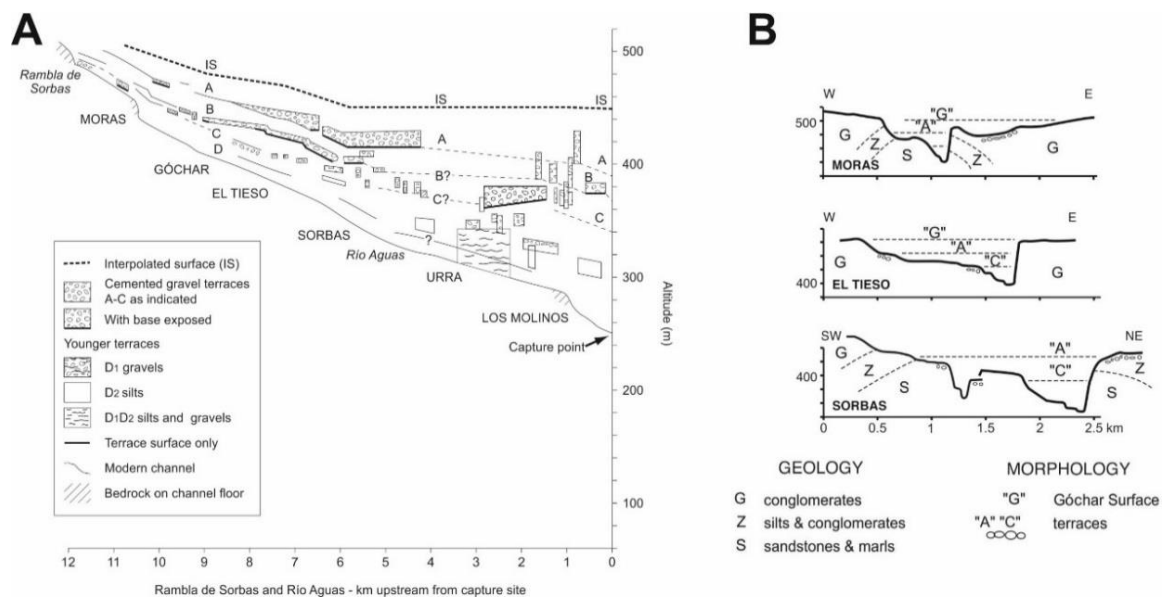
Figure 5. (**A**) River long profile and terraces of the (upstream) Rambla de Sorbas and (downstream) Río Aguas (modified from [10]). Marked steps in the Gochar surface and terraces A-C profiles around Sorbas relate to rock strength variations and a change in drainage orientation. (**B**) Cross valley profiles to illustrate the top basin surface (Gochar surface) and its relationship to key inset river terrace levels (modified from [10]).

The surface studied here is stratigraphically positioned between the Gochar Formation and Level A of the Pleistocene river terrace sequence (Figures 3–5) and is likely to be of Quaternary age based on relative dating. Similar high elevation surfaces occur in adjacent intramontane basins (Huércal-Overa, Vera, Tabernas: Figure 1) where they cap the basin fill and mark the onset of basin incision [16,39,40]. Similar surfaces with varying degrees of expression and quality of preservation are noted throughout the Betic Cordillera Internal Zone region where they are considered as an indicator of the most recent phase of relief generation within the Betics [41]. In the Sorbas Basin, the surface is fragmentary but appears to be a single and spatially extensive feature, comprising a series of rounded ridge crests and hilltops, developed primarily onto the Gochar Formation. Here, we focus on the most extensive surface remnants associated with the Gochar Formation outcrop.

3. Methods

3.1. Surface Morphology

We describe the top basin surface morphology using a combination of field and remote sensing approaches. The general surface configuration is imaged from different basin margin perspectives using elevated view points and oblique aerial drone imagery. Remote sensing of the surface used digital datasets, interrogated within Arc Map 10.5.1 (Esri, Redlands, CA, USA). The basin-scale outcrop of the Gochar Formation used digitized 1:50,000 geological maps [25,26]. The broader basin geomorphology used 5 m DEM data sourced online [42] with checks against other commonly used datasets (e.g., SRTM) to ensure visualization and analysis quality [43].

The top basin surface is an erosional feature that lacks any sedimentary deposits. As such, the surface remnants are preserved in the rounded ridge crests and hilltops within the highest elevation areas of the Gochar Formation outcrop (Figure 6).
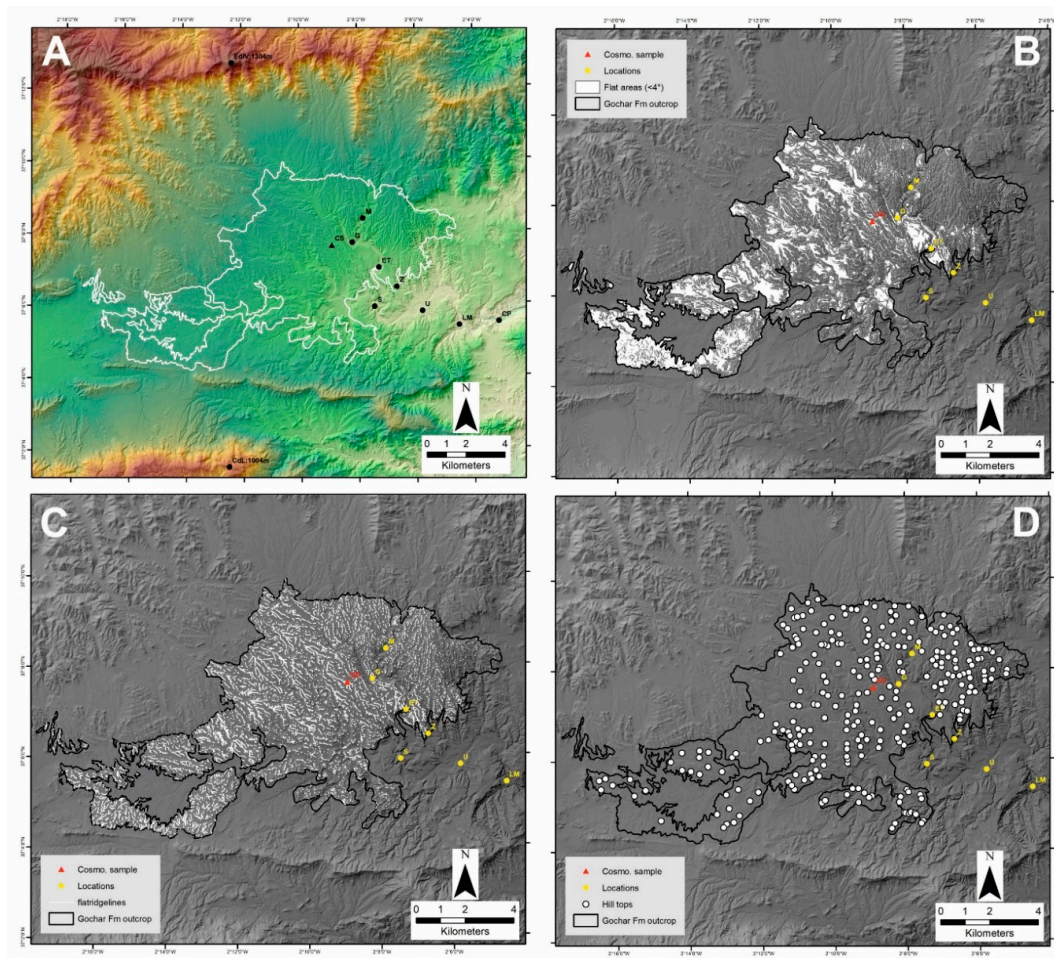
Figure 6. (**A**) DEM and hillshade showing Gochar Formation outcrop and key locations. (**B**) Slope map of areas of <4°. (**C**) Ridge lines within the Gochar Formation outcrop. (**D**) Final dataset of the highest elevation hilltops used for surface interpolation.

To map these areas, hilltop locations and elevations were combined with flat ridge crest regions. The assumption is that these highest-flattest ridges are the most representative surface remnants, since steeper dipping and lower elevation ridges will have been formed by incision into the top basin surface. Hilltops were extracted from spot heights using scanned 1:25,000 topographic maps [42] in combination with the 5 m DEM. Hilltops were removed from the dataset if (1) the spot height coincided with lower level inset river terrace locations (cross-referenced by using a combination of published terrace maps [10,35], terrace capping red soil regions identified from satellite imagery, and cross-valley profiles); (2) had no proximity relationship to the high elevation flat ridge areas (see below); (3) were anomalously low/high elevation occurrences compared to adjacent spot heights and (4) where the difference between the spot height and DEM elevation value was >5 m. Ridge crests were obtained from the DEM using an inverse stream extraction approach [44]. A reclassified slope map was then used to capture the flattest ridges (i.e., ridges coinciding with slopes of <5°). Hilltops that coincided with the flat ridges were then used as interpolation points from which to reconstruct the top basin fill surface.

3.2. Surface Reconstruction and Erosion Quantification

Digital surface reconstruction is a common geomorphological method for analysis of erosional landscapes at a range of spatial and temporal scales [45–48]. In this study we used the variable Inverse Distance Weighting (IDW var) approach [49] due to similarities of basin scale, landscape morphology

and higher quality of method statistical performance. Digital points from the cleaned hilltop dataset (see above) were used for the interpolation. The IDW var interpolates between known points giving greater weights to points closest to the prediction location, with weights diminishing with distance away from the known points. The interpolation was extrapolated outside of the Gochar outcrop into the basin margin mountain reliefs to explore the wider configuration of the surface, noting that interpolation accuracy would have diminished due to the nature of IDW var method. The resultant interpolated top basin surface was combined with the modern landscape DEM to allow analysis of areas above and below the interpolated surface (a DEM of Difference). We consider the original top surface to dip towards the basin centre and to have an undulating morphology based on erosion due to lithological and tectonic substrate heterogeneities onto which the surface was developed. Surface hilltops (*N* = 278) within the Gochar Formation outcrop range from 582 m to 442 m with a mean elevation of 511 m and average distance between hilltops of 273 m. Elevations between groups of adjacent hilltops is typically <10 m. In areas adjacent to the river valleys the hilltop elevations (i.e., the surface remnants) range from 10–20 m above terrace level A (Figure 5). Thus, a buffer value of ±10 m was used to reclassify the DEM of Difference to model the extent of the top surface that is preserved within the modern landscape.

The interpolated top basin surface was used to assess the amount of erosion that has taken place since surface formation. Erosion was calculated by subtracting the interpolated surface from the modern landscape DEM. Since surface formation, the Sorbas Basin catchment area has been modified by capture-related drainage network re-organization [24] and we therefore use the Aguas-Feos capture site as the downstream limit for the erosion calculation (Figure 2, Figure 4, and Figure 5).

3.3. Surface Dating

Dating of the top basin surface was undertaken using a ^{10}Be-^{26}Al cosmonuclide depth-profile originally sampled and analysed by Ilott [38] as part of a broader chronological investigation of the timing of Quaternary fluvial landscape development within the Sorbas Basin. The paired isotope and depth-profile approach allowed for surface exposure and burial age quantification [50]. The surface exposure technique measures the concentration of cosmonuclides at the surface [51], with concentrations affected by the time of exposure to cosmic radiation, cosmonuclide loss due to erosion, sediment density variability (affects cosmic ray attenuation) and cosmonuclide production variations [15,52]. Burial dating uses known radioactive decay rates of cosmonuclides and requires analysis of samples shielded (deep burial) from cosmic radiation after exposure [53], but with potential problems concerning cosmonuclide inheritance issues related to complex exposure-burial histories prior to deposition [54,55].

Sampling was undertaken on a road cutting (37.12692 −2.148214) that passed through one of the higher elevation flat ridges (~495 m) developed into Gochar Formation conglomerates in a north-central basin location (Figure 2). The section comprises ~2.5 m of massive and variably cemented gravel-cobble conglomerate capped by a 0.4 m soil unit, comprising a 0.1 m laminar calcrete and overlying 0.3 m red soil (Munsell = 7.5YR/4R). Sampling was undertaken up the section face at 0.5 m intervals from 2 m depth to the surface with >30 quartz clasts of >5 cm length sampled for each interval. The section location, aspect, angle of section repose, angle to highest topographic feature and surface altitude were quantified for data modelling inputs. The samples were crushed and milled, etched with HF for cleaning followed by dissolution, chemical separation (anion exchange and hydroxide precipitation) and a final metal mixing before AMS measurement.

The original age modelling [38] was undertaken using the CRONUS calculator [56] within Matlab (MathWorks, Natick, MA, USA). The concentration results revealed no hiatus within the profile so a simple exposure history was explored. This involved using a Chi square minimization method that was applied to the raw nuclide concentration data to allow fitting to the accumulation model equations of Lal [57] with variable inheritance, density and erosion data input values [15,50].

For the purpose of this study we remodelled the concentration data using the updated CRONUS 2.3 calculator [58]. New surface erosion estimates of 10 m and 4 m were inputted to represent the relationship of the cosmogenic sample site to the interpolated surface (see results). A value of 10 m was used to reflect the general elevation range between adjacent hilltop heights used for surface interpolation. A value of 4 m was also used as this is the height of the sample site below the interpolated surface. An average upstream altitude of 689 m was derived from the 5 m DEM as a modelling data input to improve the maximum burial age value.

Maximum and minimum exposure and burial ages were calculated. These values were considered alongside other published age data for the region to inform on the timing of surface formation. Combination of the remodelled ages with surface incision data enabled amounts and rates of basin erosion to be calculated.

4. Results

4.1. Surface Morphology and Erosion

The field expression of the surface is shown from a range of basin margin perspectives in Figure 7. The surface comprises high elevation isolated hilltops and gently dipping but discontinuous ridge crests, with numerous intervening topographic lows along the ridge lengths and between adjacent hilltops. The hilltops and ridges are further accentuated by incision of the modern drainage network and its tributaries. Despite the erosion, the various landscape panoramic perspectives and along ridge slope profiles (Figure 7) clearly demonstrates a visual correlation and reconstruction of a single surface in a downslope basin centre direction.

Reconstruction of the surface using IDW var interpolation of the hilltop dataset within the Gochar Formation outcrop shows that the top basin surface is contained almost entirely within the broader sedimentary infill of the Sorbas Basin (Figure 8). The surface is particularly prevalent in northern, central and western regions, with low preservation in the south (Figure 8). Areas eroded below the surface coincide with the modern drainage network, concentrated along the major tributary valleys and becoming widespread towards the east along the Río Aguas as it routes into the Vera Basin (Figure 9). Other extensive areas below the surface occur in the headwaters of the Tabernas Basin (west) and the Carboneras-Almería Basin (south). Areas above the surface are mainly concentrated in the mountains of metamorphic basement that border the Sorbas Basin, but there are notable areas where Miocene basin fill sediments form topographic highs within the west and south of the basin. When compared to the modern Río Aguas catchment upstream of the capture site (285 km^2), the maximum extent of the interpolated surface covers 144 km^2, some 50% of the modern catchment. The amounts of incision below the interpolated surface increase downstream to a maximum of -254 m (Figure 9) with a mean basin surface lowering of ~31 m. This incision is concentrated along the lower reaches of tributaries draining to the basin centre and downstream along the main Rio Aguas valley, especially between Sorbas and the capture point east of Los Molinos. The volume of sediment removed by the erosion is 5.95 km^3.

The areas of better surface preservation are associated within the confines of the Gochar Formation outcrop. Within this region, the interpolated surface comprises an area of 35 km^2, some 44% of the Gochar Formation outcrop. The hilltops, ridges of the interpolated surface and the incised drainage pick out a series of relict fan-shaped bodies (Figure 10) that broadly correspond to the dip slopes of the synclinal fold configuration of the Sorbas Basin (Figure 2). These are most evident along the northern basin margin, comprising at least two fans of 5–6 km length that backfill into the embayed Sierra de los Filabres mountain front (Figure 10). The clearest of the fans, the eastern 'Cariatiz Fan' (Figure 10B), was used by Mather et al. [59] as part of a regional morphometric study of modern and older Plio-Quaternary fans in SE Spain to illustrate the importance of capture-related re-organizations of fan source areas.
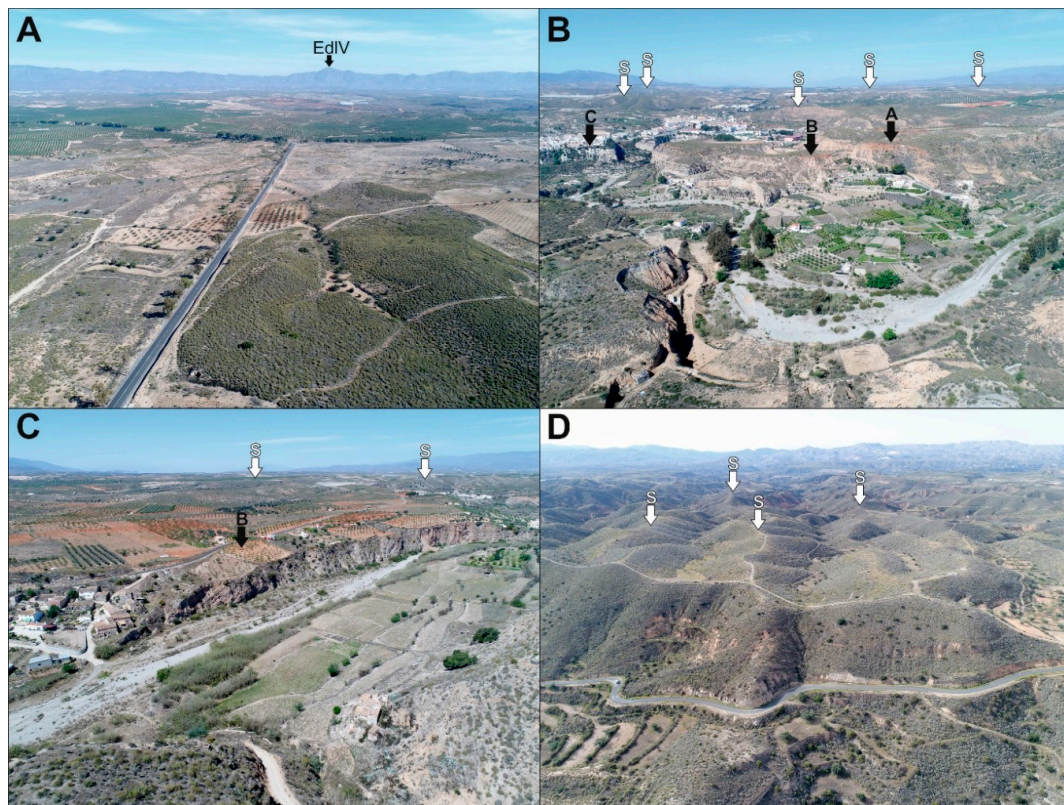
Figure 7. Field imaging of relict surface. (**A**) View from south western basin margin (37.06899 −2.19864) looking north across the basin surface with little dissection. EdlV = Ermita de la Virgen 1304 m. (**B**) View from southeastern basin margin (37.10498 −2.11419) looking west across the Rambla de Sorbas inset terrace sequence (A, B, C) in the Sorbas town region. Surface remnants (S) visible in distance. (**C**) View from eastern basin margin (37.12254 −2.11848) looking northwest across the El Tieso 'B' terrace with extensive surface remnants visible in far ground (S). (**D**) View south-southwest from the northeastern basin margin (37.145648 −2.099306) along ridgelines of the relict surface (S).
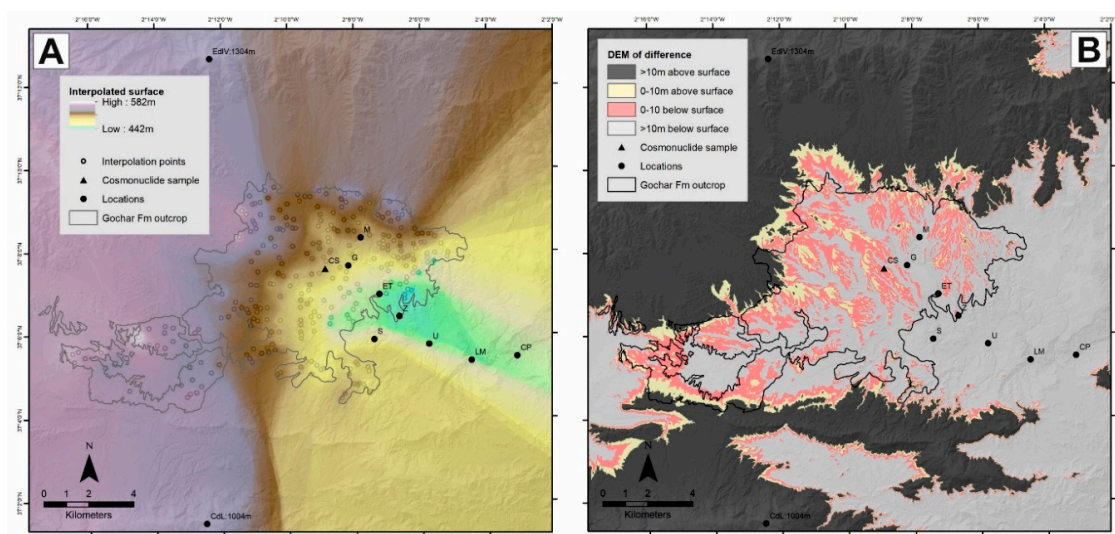

Figure 8. (**A**) Interpolated surface results. (**B**) Comparison of the interpolated surface with the modern landscape highlighting areas that are 10 m above and below the interpolated surface.
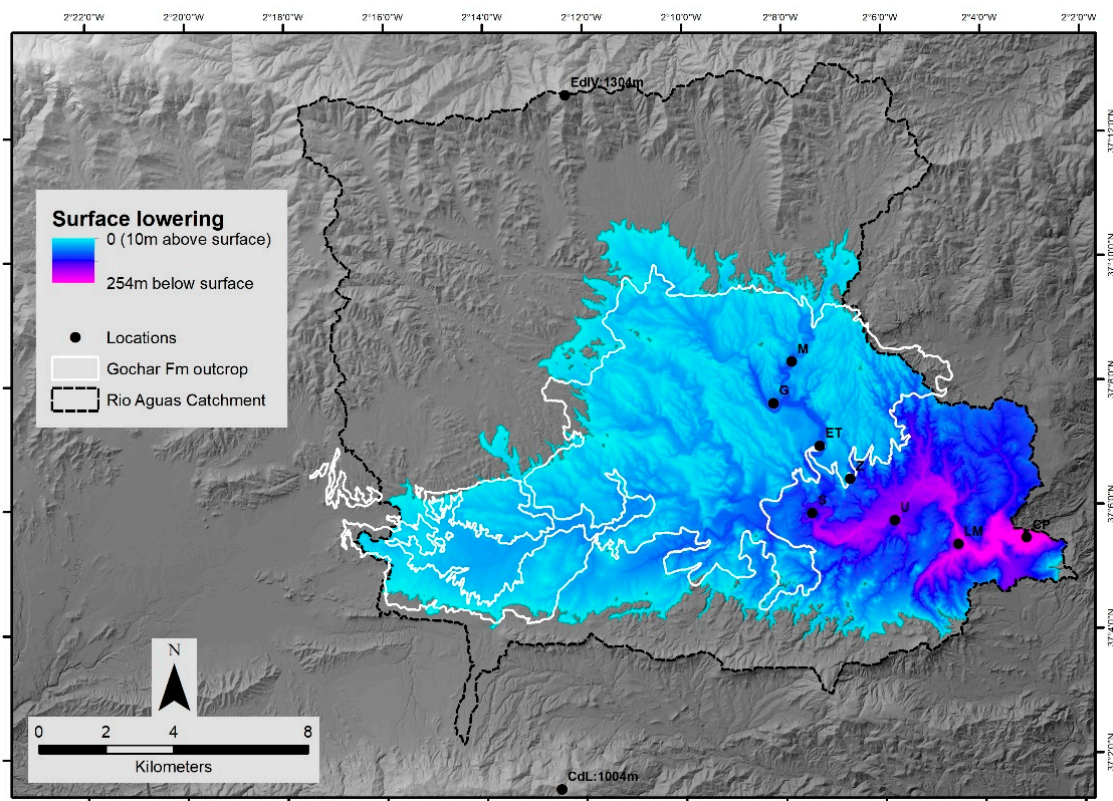
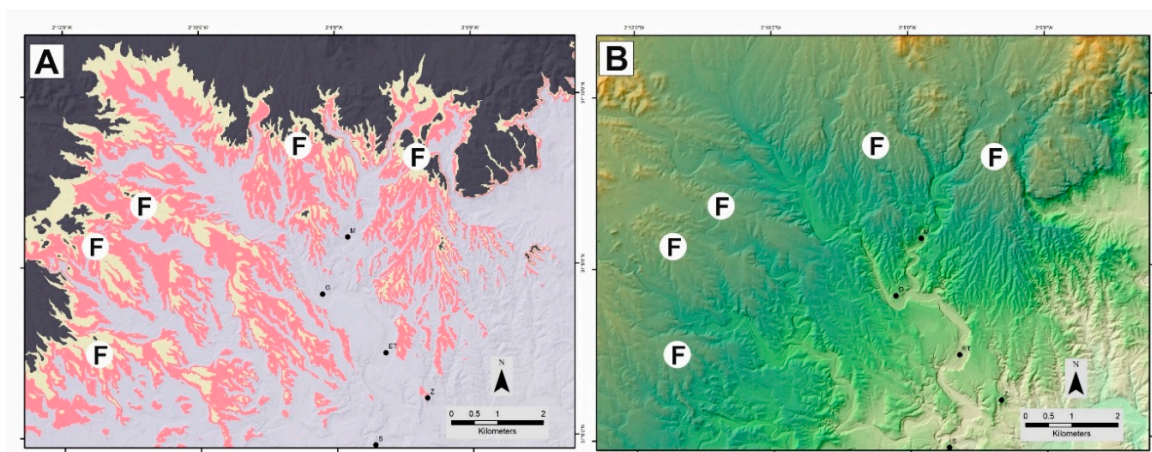**Figure 9.** Surface lowering map showing concentrated erosion in the east and upstream along tributary channels.

Figure 10. Fan-shaped geometries (F) enhanced by surface interpolation (**A**). Modern landscape DEM (**B**) for comparison. Cariatiz Fan = NE fan.

A series of 4–7 km long fans are also evident along the western and northwestern basin margins, but their morphology is less clear. The surface interpolation (Figure 10) accentuates these fan features suggesting that the formation of the surface erosion and its subsequent incision is accentuating and exploiting the Gochar Formation palaeogeography and its drainage morphology of the Marchalico and Gochar systems [20]. Fan morphologies are not evident in the surface remnants along the southern basin margin, possibly reflecting a more fragmentary surface record or that the higher uplift rate and greater degree of deformation along the southern basin margin [60] has destroyed any Gochar Formation drainage morphology in that area.

4.2. Surface Age and Erosion

The cosmonuclide sample site location examined by Ilott [38] is located on a gently dipping NW-SE orientated ridge with rounded edges that slope into an adjacent incised drainage network that visually appears to be part of the relict surface. Within the broader landscape, the sampled ridge is slightly inset when compared to adjacent ridge hilltop elevations (Figure 11). The interpolation modelling confirms the inset configuration (Figure 11), with the site occurring at −4 m below the interpolated surface and within the broad −10 m buffer zone (see Section 3). As such, the sample site does not provide the best representation of the 'true' surface but instead relates to the onset of incision into it. However, this incision amount is too small for the sampled ridge to be part of terrace Level A, which is typically positioned at 20 m below the interpolated surface (Figure 5). A benefit of knowing surface and terrace elevation variability is that the values provide erosion data inputs for modelling the cosmonuclide exposure and burial ages (see Section 3).

The remodelled cosmonuclide data are presented in the Supplementary Materials and summary results in Table 1. Using the higher 10 m erosion value provides exposure ages of 1990 ka (maximum) and 169 ka (minimum) and burial ages of 1056 ka (maximum) and 679 ka (minimum). In contrast, using a 4 m erosion value provides exposure ages of 798 ka (maximum) and 169 ka (minimum) and burial ages of 1048 ka (maximum) and 679 ka (minimum). These ages span the Early-Middle Pleistocene (maximum exposure-burial ages) and Middle-Late Pleistocene (minimum exposure-burial ages). Stratigraphic convention should mean that the sediment (burial) age should be older than that of the surface (exposure) age. However, the age inconsistencies are explainable as they reinforce the surface origin as an erosional form as opposed to a depositional top basin fill surface. Furthermore, despite the age variability, the results provide some insight into the broad timing of surface formation. The minimum 679 ka burial ages suggest that surface is older than 679 ka and probably more in keeping with the Early Pleistocene. Indeed, the more realistic surface age scenarios are probably closer to the maximum burial age range 1056–798 ka for both the erosion amount scenarios. An Early Pleistocene surface age is also supported by the chronologies of the inset river terrace sequence where U-Series dating of pedogenic terrace capping calcretes show that terraces A and B are Middle Pleistocene landforms [36,37].

Table 1. Remodelled cosmonuclide exposure and burial age results. See Supplementary Materials for detail.

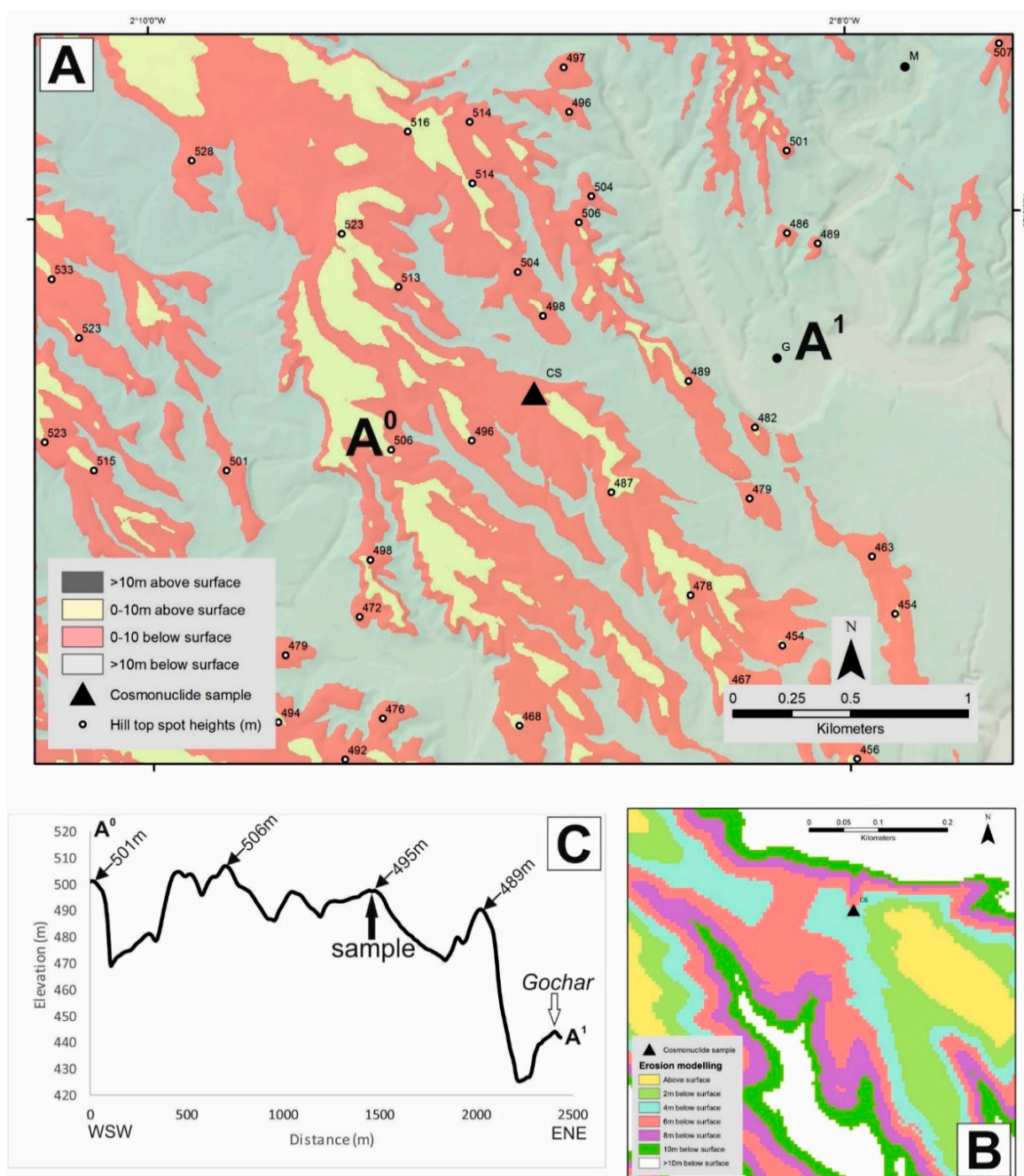| Surface erosion (m)	Min. exposure age (ka)	Max. exposure age (ka)	Min. sediment burial age (Ma)	Max. sediment burial age (Ma)	Min. surface erosion rate (m/Ma)	Max. surface erosion rate (m/Ma)	Min. upstream basin erosion rate (m/Ma)	Max. upstream basin erosion rate (m/Ma)	Reduced chi-square	Min. depositional age (ka)	Max. depositional age (ka)
10	169	1990	0.679	1.056	0.04	5.98	6.8	9.3	2.8	191	1056
4	169	798	0.679	1.048	0.05	5.72	6.6	8.7	2.9	191	798

Figure 11. Visualization of the interpolated surface at 10 m (**A**) and 2 m (**B**) intervals, showing that the cosmonuclide sample site is located ~4 m below the interpolated surface. (**C**) Topographic profile further illustrating the inset nature of sample site.

The AMS measurements collectively revealed high concentrations of inherited [10]Be and [26]Al (Supplementary Materials) and this begins to inform on the transport history and relative landscape stability of the end Gochar Formation period prior to surface formation. It suggests that sediments were generated under low basin erosion rate conditions, implying a relatively stable landscape with recycling of the basin fill most likely from the Gochar Formation sediments into which the surface has developed [19].

The cosmonuclide age data can be combined with the interpolated surface to provide insights into rates of basin erosion. Because the surface is most likely Early Pleistocene (see above discussion)

we use the maximum and minimum burial ages in conjunction with the surface lowering (~31 m) and volume (5.95 km^3) data to calculate the surface lowering and volume erosion rates. Surface lowering rates range from 46 mm/ka (minimum burial age: 679 ka) to 29 mm/ka (maximum burial age—10 m: 1056 ka). Volume rates range from 0.001 km^3/ka (minimum burial age: 679 ka) to 0.004 km^3/ka (maximum burial age—10 m: 1056 ka).

5. Discussion

5.1. Controls on Surface Formation

Despite the fragmentary nature of high elevation hilltops and ridges within the Sorbas Basin, they link together to form a single surface developed across the basin fill. Its crosscutting relationship with the underlying Gochar Formation suggests it represents a key basin wide erosional event that marks the onset of basin incision. The erosion has cut across deformed Gochar Formation sediments, meaning that surface construction post-dated a basin wide deformation event. Although surface remnants form a single surface that grades from the basin margins to the basin centre there are local elevation differences between adjacent surface remnants. These differences may relate to variations in strength, stratigraphy and localised deformation of the basin fill or a passive exploitation of the basin fill palaeogeography and its relict morphology of the depositional environment. For example, surfaces developed into flat lying and fine grained lacustrine dominated intramontane basin infills (e.g., Guadix-Baza [11]) are more likely to be well developed and spatially extensive than those developed into dipping and coarse-grained alluvial intramontane basin fills (this study).

Surfaces are evident throughout Betic Cordillera intramontane basins (Figure 12), occupying mountain fronts where surface remnants dip towards the basin centre [13]. These surfaces are either (1) degraded forms, lacking in sediment cover and developed onto the Plio-Pleistocene continental alluvial basin infill (e.g., Sorbas Basin) or (2) are well preserved, with a <20 m thick cover of coarse-grained alluvial conglomerates, that unconformably overlie Neogene marine basin infill (e.g., Tabernas and eastern Vera Basin) (Figure 12). The well-preserved surfaces often comprise a pedogenic calcrete cap, with groundwater calcretes sometimes developed along the basal unconformity contact [14,61]. Although surfaces may have origins associated with alluvial fan environments [13], they are more typical of pediments (sensu King [62]) that have been observed worldwide, with examples throughout SE Spain often referred to using the French term 'glacis' [63]. The degraded surface considered here could be a highly eroded pediment remnant, most likely a bedrock pediment or the remnants of the bedrock base of a pediment due to absence of calcrete and alluvial cover. Studies of pediment formation [64] suggest they form at mountain fronts where bedrock weathers to sediment; in climates with a soil hydrology, vegetation cover and weathering style that suppresses fluvial incision and deep bedrock weathering; and a balanced mountain front sediment flux and base level position. If the top basin surface follows these criteria for autogenic formation, then the surface informs indirectly on Quaternary climate and tectonics. The climatic criteria are fulfilled due to a persistence of seasonally variable cool/warm dryland climatic conditions throughout the Quaternary [65–68]. However, the base level configuration has changed, particularly with respect to the top basin surface as it marks a key point at which the basin switches from sedimentation to erosion, after which there is a sustained base-level lowering linked to tectonic uplift and capture [13,69]. For the top surface to form as a basin wide feature means that dryland conditions must have coincided with a stable and sustained basin level position during a time of relative tectonic quiescence and a time when the drainage network configuration was not conducive to capture. Uplift rate quantifications for the Sorbas Basin are time averaged from the lower Pliocene (70–160 m Ma^{-1}: [19,69]) and thus lack temporal clarity to inform on the restricted pediment formation timescale. However, direct evidence for deformation is restricted to the Gochar Formation sediments into which the surface is developed, implying a marked reduction in tectonic activity at the time of surface formation and thus base level stabilization. Tectonics would have also played a passive role in surface formation, with the

overall basin syncline configuration forming fold limb dip slope drainages routed to a basin centre axial drainage coincident with the basin syncline axis. Subsequent fluvial incision appears to have concentrated along the synclinal axis, dissipating upstream along the fold limb configured streams (Figures 8 and 9). The passive influence of fold structures on drainage pattern configuration and development is a commonly reported feature in collisional mountain belt settings [70].
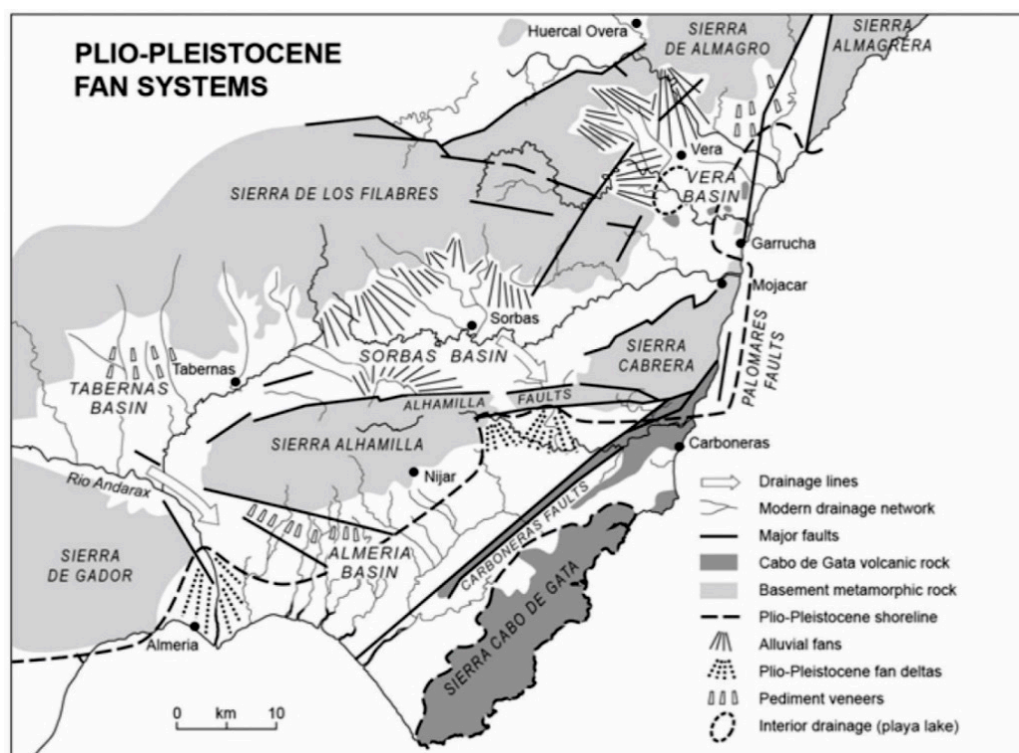

Figure 12. Regional occurrence of Plio-Pleistocene alluvial fan/pediment systems within the east-central Betic Cordillera [13]. Degraded surfaces are developed onto Plio-Pleistocene continental (alluvial fan) sediments, whilst well preserved surfaces (pediment veneers) are developed onto Neogene marine sediments.

The very nature of the surface as a continuous basin wide feature implies the absence of an incised drainage network for it to form by autogenic processes, e.g., [64]. Drainage routing throughout the Plio/Quaternary has recorded a persistent pattern of basin margin streams feeding an axial drainage [12,20,24]. Because the surface has formed as an interval in-between the final basin infilling and pre-basin incision, it too is likely to have formed by the same basin convergent drainage pattern (Figure 12). If the basin was undissected then radiating streams with collective fan-shaped forms would have dominated the palaeogeography (in-keeping with the Gochar Formation), with autogenic lateral shifting of the radiating streams being responsible for creating the pediment like surface, noting that any pediment cover sediments are not preserved due to the eroded/degraded surface form. The surface remnants and interpolation mapping (Figure 10) provides strong evidence for large fan-shaped bodies along the northern and western basin margins. These morphologies, particularly along the northern margin, are accentuated because of progressive surface incision and localised captures.

Headwards erosion by the axial drainage has exploited the inter-fan drainage areas (Figure 13). It is common for alluvial fans to develop an incised drainage along their axial feeder channel due to a connectivity interplay between fan head and fan toe base-level variations [71]. Because incision and headwards erosion has been concentrated along the interfan areas it suggests that the fans responsible for autogenically creating the surface were undissected with insufficient axial drainage to be exploited. As headwards erosion has proceeded up the interfan areas it has captured the fan feeders, resulting in

fan abandonment [72]. The fans forming the pediment surface would have also possessed an overall convex morphology with topographic lows present within interfan areas. This convex morphology may have also played a role in passively influencing interfan drainage exploitation.
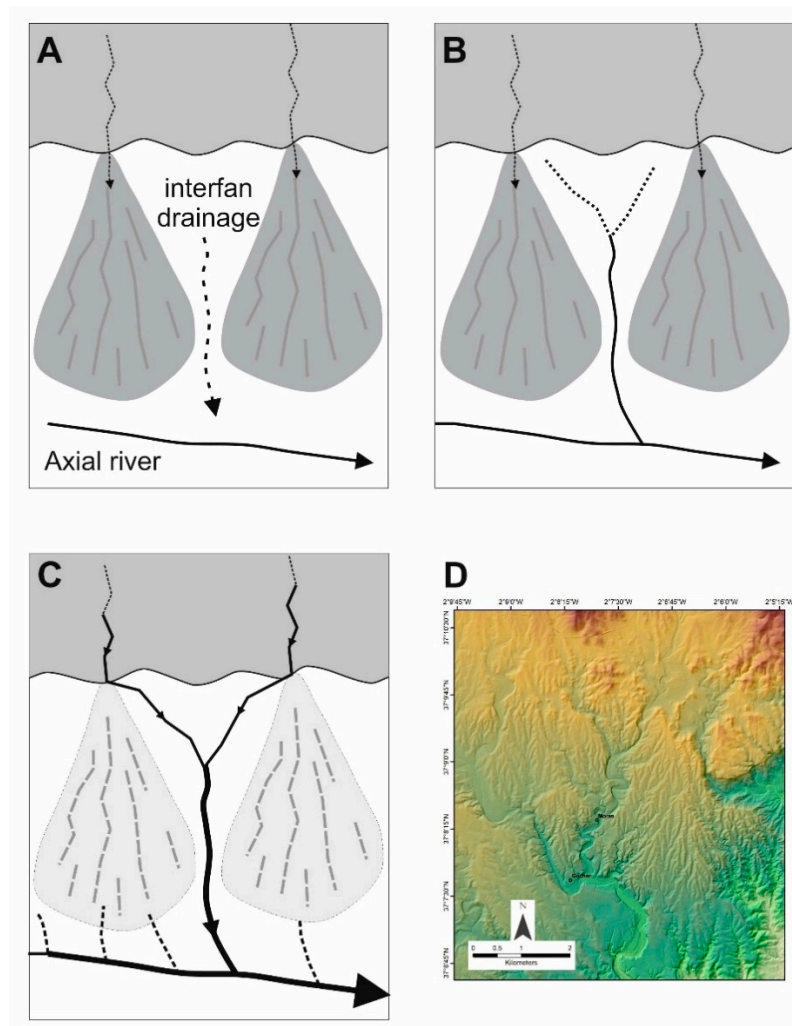

Figure 13. Fan/pediment abandonment model based on Sorbas Basin northern margin. (**A**–**C**) Interfan development and capture of mountain front fan feeder streams. (**D**) Relict fan morphology with former interfan drainage now forming a key component of the current drainage network.

5.2. Timing of Surface Formation

The remodelled cosmonuclide data suggest that the surface is an Early Pleistocene feature, with the max-min burial ages (1056–679 ka: Table 1) providing the most coherent age range indicators for surface development. This means that the underlying Gochar Formation into which the surface is developed spans the Pliocene and probably the earliest Pleistocene based upon bracketing between a basal Mio-Pliocene boundary age [30] and a top Early Pleistocene age (this study). From a geological perspective the Early Pleistocene surface age presented here is significant for understanding the Late Miocene geological history of the Sorbas Basin which has received considerable attention for its role in documenting the Mediterranean Messinian Salinity Crisis. Clauzon et al. [31] describe the same surface studied here (see Figure 8G in [31], and Figure 7C of this study) as a fan-delta abandonment feature assigning a Mio-Pliocene (~5.3 Ma) boundary age to the surface through downslope extrapolation to a biostratigraphically dated Zorreras Member type location section, the Zorreras Hill (Figure 2). This 450 m elevation hilltop is capped by Gochar Formation conglomerates

and fits within our interpolated surface dataset. However, its Early Pleistocene cosmonuclide age bears no relationship to the immediate post Messinian Salinity Crisis recovery of the Sorbas basin as implied by Clauzon et al. [31].

The regional significance of the style and timing of Sorbas Basin surface formation within the Betic Cordillera can be further explored through comparison with adjacent intramontane basins (Figure 12). To the east, the Vera Basin is like Sorbas, comprising a deformed continental basin infill (Salmerón Formation) that grades into a high elevation pediment surface and an inset fan pediment-river terrace sequence [73–75]. Electron Spin Resonance (ESR) dating brackets the Salmerón Formation and its pediment to the Early Pleistocene (~2.4–1.3 Ma) [76,77]. The timing appears co-eval with the latter stages of the Gochar Formation, attributed to regional uplift timing and amount variability between the Sorbas (earlier and greater uplift) and Vera Basins [40]. The inset Vera Basin pediment-river terrace sequence spans the Middle to Late Pleistocene based upon ESR and OSL chronologies [78,79]. This timing is in-keeping with the U-Series dated Middle-Late Pleistocene Sorbas Basin river terrace sequence [36,37]. Other adjacent basins (Huércal-Overa, Tabernas, Carboneras-Almería) show varying degrees of geological-geomorphological similarity: (1) Pliocene-Early Pleistocene basin fill, (2) Early Pleistocene deformation and (3) Middle-Late Pleistocene pediment-river terrace sequence formation [16,39,50]. Farines et al. [41] attributes the Early Pleistocene to the most recent phase of Betic Cordillera relief generation, highlighting a poorly understood interplay between mechanical and isostatic relief building processes, with ductile crustal flow cited as a key Plio/Quaternary uplift mechanism. Of note, is the Guadix-Baza Basin, the largest and most intensively studied intramontane basins in the region. This basin occupies a central-interior location within the Betics and differs in timing to Sorbas and its adjacent basins. The Guadix-Baza Basin is characterised by a continuous Miocene-Late Pleistocene continental sedimentary infill [68], capped by a single Late Pleistocene pediment into which extensive basin wide erosion has occurred following capture by the Río Guadalquivir sometime between 350 to 68 ka [4,47]. This difference in timing and pattern of basin geological-geomorphological development reflects variations and connectivity of regional base-levels. Sorbas and adjacent basins occupy marginal mountain belt locations with better connectivity to the Mediterranean coastlines, thus responding more effectively to regional base-level change. In contrast, the Guadix-Baza Basin has an interior mountain belt location with an internal drainage disconnected from regional base-level variability, until captured very recently geologically speaking.

High elevation Early Pleistocene pediment surfaces are also present within intraplate basins as part of the largest drainage systems in Iberia such as the Duero and Tajo [80]. These surfaces have alluvial fan origins and show development within wide-shallow valleys that form the beginnings of river terrace staircases that record hundreds of metres of incision [80]. Thus, the Early Pleistocene is an important interval for surface development and a key marker for subsequent fluvial landscape incision, both within the Betic Cordillera (this study) and within Iberia [81]. Climate and base level (tectonic and capture) variability are widely cited controlling mechanisms for Early Pleistocene Iberian landscape development [48,80–82]. Surface formation within the Sorbas Basin clearly demonstrates interplay of these factors, but the surface itself probably reflects a sustained period of climate stability and base level position to allow the surface to form autogenically at a basin scale. Marked changes to the global climate [83] and regional base levels [12,41] are then driving the surface abandonment and incision.

5.3. Basin Erosion

The interpolation derived basin erosion rates quantified in this study (Figure 9) can be compared with erosion of the Sierra de los Filabres using ^{10}Be [84]. Rates of 52 ± 6 mm/ka were derived from basement schist dominated catchments of tributaries to the Río Jauto along the northeastern margin of the Sorbas Basin [84]. These catchments were formerly part of the main Sorbas Basin drainage before being captured and routed to the southern Vera Basin sometime during the Middle-Late Pleistocene [12]. The average basin surface lowering rates calculated in this study using the dated

interpolated surface cover a lower range at 29–46 mm/ka. This could be due to rock strength differences between variably cemented conglomerate basin infill (this study) vs easily weathered basement schist [84]. However, the low value from the Sorbas surface is still broadly in keeping with Betic Cordillera mean (64 ± 54 mm/ka^{-1}), reflecting low tectonic uplift and possibly a steady state topography where denudation balances uplift [84].

6. Conclusions

- Despite a fragmentary nature, the top Sorbas Basin surface can be reconstructed using GIS interpolation (IDW var) where a sufficiently high-resolution DEM is available;

- The surface is an erosional pediment (glacis) form and not the depositional surface of the Gochar Formation;

- The surface is an Early Pleistocene feature, developed onto deformed basin fill;

- The surface reconstruction approach used here could be used to inform on sampling strategy for dating or could help clarify local surface erosion for age modelling purposes;

- The basin wide configuration of the surface suggests surface formation by autogenic processes that are operating within a stable landscape characterized by a sustained dryland climate and fixed base-level;

- The relict fan-morphology picked out by the surface remnants suggests the surface was autogenically eroded by undissected radiating mountain front streams that formed fan-shaped bodies;

- The Early Pleistocene surface age helps stratigraphically bracket the underlying Gochar Formation to the Pliocene. This clarifies the degraded pediment surface as a Quaternary landscape feature and not a Mio-Pliocene fan delta abandonment surface linked to the post Messinian salinity crisis recovery;

- Surface abandonment took place during the Middle Pleistocene with preferential incision along interfan drainage lines, resulting in capture to preserve the relict fan morphologies;

- Early Pleistocene surfaces are evident throughout Betic Cordillera intramontane basins as either (1) well developed pediments, developed onto Neogene marine basin fill sediments (e.g., Tabernas, Vera Basins) or (2) degraded pediments developed onto Plio-Pleistocene continental alluvial basin fill sediments (Sorbas Basin). Collectively these pediments are regionally and temporally significant, with formation occurring during a stable phase that post-dates deformation of the Plio-Pleistocene continental sediments that form the final basin infill. The deformation and subsequent surface formation probably correspond to the most recent major uplift and relief building phase of the Betic Cordillera;

- Surface form reflects differences in substrate lithology, passive basin tectonic configuration and depositional setting (e.g., lake vs fan);

- Regional variations in surface preservation and differences in formation timing relates to base-level connectivity with the Mediterranean coastal margins of the Betic Cordillera;

- Surface lowering and erosion amounts, and rates are low, comparing well with other denudation techniques (e.g., ^{10}Be) and are in keeping with the Betic Cordillera as a low uplift rate mountain range. The base-level lowering since surface formation is probably an ongoing response to the low uplift rates and basin scale capture events.

Author Contributions: Conceptualization, M.S. and A.E.M.; Methodology, M.S., A.E.M., Á.R., S.L.; Software, Á.R., S.L.; Validation, M.S., Á.R., S.L.; Formal Analysis, M.S., Á.R., S.L.; Investigation, M.S., A.E.M., Á.R., S.H.K., S.L.; Resources, Á.R., S.L.; Data Curation, M.S., Á.R.; Writing—Original Draft Preparation, M.S.; Writing—Review

References

1. Kingston, D.R.; Dishroon, C.P.; Williams, P.A. Global basin classification system. *AAPG Bull.* **1983**, *67*, 2175–2193.

2. Sanz De Galdeano, C.; Vera, J.A. Stratigraphic record and palaeogeographical context of the Neogene basins in the Betic Cordillera, Spain. *Basin Res.* **1992**, *4*, 21–35. [CrossRef]

3. Sobel, E.R.; Hilley, G.E.; Strecker, M.R. Formation of internally drained contractional basins by aridity-limited bedrock incision. *J. Geophys. Res.* **2003**, *108*. [CrossRef]

4. Calvache, M.L.; Viseras, C. Long-term control mechanisms of stream piracy processes in southeast Spain. *Earth Surf. Process. Landf.* **1997**, *22*, 93–105. [CrossRef]

5. Craddock, W.H.; Kirby, E.; Harkins, N.W.; Zhang, H.; Shi, X.; Liu, J. Rapid fluvial incision along the Yellow River during headward basin integration. *Nat. Geosci.* **2010**, *3*, 209–213. [CrossRef]

6. Soria, J.M.; Fernández, J.; Viseras, C. Late Miocene stratigraphy and palaeogeographic evolution of the intramontane Guadix Basin (Central Betic Cordillera, Spain): Implications for an Atlantic–Mediterranean connection. *Palaeogeogr. Palaeoclimatol. Palaeoecol.* **1999**, *151*, 255–266. [CrossRef]

7. Benvenuti, M.; Bonini, M.; Moroni, A. Tectonic control on the Late Quaternary hydrography of the Upper Tiber Basin (Northern Apennines, Italy). *Geomorphology* **2016**, *269*, 85–103. [CrossRef]

8. Watchman, A.L.; Twidale, C.R. Relative and 'absolute'dating of land surfaces. *Earth-Sci. Rev.* **2002**, *58*, 1–49. [CrossRef]

9. Viseras, C.; Fernández, J. Sedimentary basin destruction inferred from the evolution of drainage systems in the Betic Cordillera, southern Spain. *J. Geol. Soc.* **1992**, *149*, 1021–1029. [CrossRef]

10. Stokes, M.; Mather, A.E.; Harvey, A.M. Quantification of river-capture-induced base-level changes and landscape development, Sorbas Basin, SE Spain. *Geol. Soc. Lond. Spec. Publ.* **2002**, *191*, 23–35. [CrossRef]

11. García-Tortosa, F.J.; Alfaro, P.; de Galdeano, C.S.; Galindo-Zaldívar, J. Glacis geometry as a geomorphic marker of recent tectonics: The Guadix–Baza basin (South Spain). *Geomorphology* **2011**, *125*, 517–529. [CrossRef]

12. Harvey, A.M.; Whitfield, E.; Stokes, M.; Mather, A. The Late Neogene to Quaternary drainage evolution of the uplifted Neogene sedimentary Basins of Almería, Betic Chain. In *Landscapes and Landforms of Spain*; Gutiérrez, F., Gutiérrez, M., Eds.; Springer: Dordrecht, The Netherlands, 2014; pp. 37–61, ISBN 978-94-017-8628-7.

13. Harvey, A.M.; Stokes, M.; Mather, A.; Whitfield, E. Spatial characteristics of the Pliocene to modern alluvial fan successions in the uplifted sedimentary basins of Almería, SE Spain: Review and regional synthesis. *Geol. Soc. Lond. Spec. Publ.* **2018**, *440*, SP440-5. [CrossRef]

14. Stokes, M.; Nash, D.J.; Harvey, A.M. Calcrete 'fossilisation' of alluvial fans in SE Spain: The roles of groundwater, pedogenic processes and fan dynamics in calcrete development. *Geomorphology* **2007**, *85*, 63–84. [CrossRef]

15. Rodés, Á.; Pallàs, R.; Braucher, R.; Moreno, X.; Masana, E.; Bourlés, D.L. Effect of density uncertainties in cosmogenic ^{10}Be depth-profiles: Dating a cemented Pleistocene alluvial fan (Carboneras Fault, SE Iberia). *Quat. Geochronol.* **2011**, *6*, 186–194. [CrossRef]

16. Geach, M.R.; Thomsen, K.J.; Buylaert, J.P.; Murray, A.S.; Mather, A.E.; Telfer, M.W.; Stokes, M. Single-grain and multi-grain OSL dating of river terrace sediments in the Tabernas Basin, SE Spain. *Quat. Geochronol.* **2015**, *30*, 213–218. [CrossRef]

17. Martín, J.; Braga, J.C. Messinian events in the Sorbas Basin in southeastern Spain and their implications in the recent history of the Mediterranean. *Sediment. Geol.* **1994**, *90*, 257–268. [CrossRef]

18. Haughton, P.D. Deposits of deflected and ponded turbidity currents, Sorbas Basin, southeast Spain. *J. Sediment. Res.* **1994**, *64*, 233–246. [CrossRef]

19. Mather, A.E. Cenozoic Drainage Evolution of the Sorbas Basin SE Spain. Ph.D. Thesis, University of Liverpool, Liverpool, UK, 1991.

20. Mather, A.E.; Harvey, A.M. Controls on drainage evolution in the Sorbas basin, southeast Spain. In *Mediterranean Quaternary River Environments*; Lewin, J., Macklin, M.G., Woodward, J.C., Eds.; Balkema: Rotterdam, The Netherlands, 1995; pp. 65–75, ISBN 9054101911.

21. IGME. *Mapa Geológico de España, 1:200 000. Almería-Garrucha, 84–85*, 2nd ed.; IGME: Madrid, Spain, 1980.

22. IGME. *Mapa Geológico de España, 1:200 000. Baza, 78*, 2nd ed.; IGME: Madrid, Spain, 1983.

23. IGME. *Mapa Geológico de España, 1:200 000. Murcia, 78*, 2nd ed.; IGME: Madrid, Spain, 1983.

24. Harvey, A.M.; Wells, S.G. Response of Quaternary fluvial systems to differential epeirogenic uplift: Aguas and Feos river systems, southeast Spain. *Geology* **1987**, *15*, 689–693. [CrossRef]

25. Vázquez, M.; Jabaloy, A.; Barbero, L.; Stuart, F.M. Deciphering tectonic-and erosion-driven exhumation of the Nevado–Filábride Complex (Betic Cordillera, Southern Spain) by low temperature thermochronology. *Terra Nova* **2011**, *23*, 257–263. [CrossRef]

26. Platt, J.P.; Kelley, S.P.; Carter, A.; Orozco, M. Timing of tectonic events in the Alpujárride Complex, Betic Cordillera, southern Spain. *J. Geol. Soc. Lond.* **2005**, *162*, 451–462. [CrossRef]

27. Giaconia, F.; Booth-Rea, G.; Martínez-Martínez, J.M.; Azañón, J.M.; Pérez-Peña, J.V.; Pérez-Romero, J.; Villegas, I. Geomorphic evidence of active tectonics in the Sierra Alhamilla (eastern Betics, SE Spain). *Geomorphology* **2012**, *145*, 90–106. [CrossRef]

28. IGME. *Mapa Geológico de España, 1:50 000. Sorbas, 1031, 24–42*; IGME: Madrid, Spain, 1973.

29. IGME. *Mapa Geológico de España, 1:50 000. Tabernas, 1030, 23–42*; IGME: Madrid, Spain, 1973.

30. Martín-Suárez, E.; Freudenthal, M.; Krijgsman, W.; Fortuin, A.R. On the age of the continental deposits of the Zorreras Member (Sorbas Basin, SE Spain). *Geobios* **2000**, *33*, 505–512. [CrossRef]

31. Clauzon, G.; Suc, J.P.; Do Couto, D.; Jouannic, G.; Melinte-Dobrinescu, M.C.; Jolivet, L.; Quillévéré, F.; Lebret, N.; Mocochain, L.; Popescu, S.M.; et al. New insights on the Sorbas Basin (SE Spain): The onshore reference of the Messinian Salinity Crisis. *Mar. Pet. Geol.* **2015**, *66*, 71–100. [CrossRef]

32. Mather, A.E. Basin inversion: Some consequences for drainage evolution and alluvial architecture. *Sedimentology* **1993**, *40*, 1069–1089. [CrossRef]

33. Griffiths, J.S.; Hart, A.B.; Mather, A.E.; Stokes, M. Assessment of some spatial and temporal issues in landslide initiation within the Río Aguas Catchment, South–East Spain. *Landslides* **2005**, *2*, 183–192. [CrossRef]

34. Mather, A.E.; Stokes, M.; Griffiths, J.S. Quaternary landscape evolution: A framework for understanding contemporary erosion, southeast Spain. *Land Degrad. Dev.* **2002**, *13*, 89–109. [CrossRef]

35. Harvey, A.M.; Miller, S.Y.; Wells, S.G. Quaternary soil and river terrace sequences in the Aguas/Feos river systems: Sorbas basin, southeast Spain. In *Mediterranean Quaternary River Environments*; Lewin, J., Macklin, M.G., Woodward, J.C., Eds.; Balkema: Rotterdam, The Netherlands, 1995; pp. 263–281, ISBN 9054101911.

36. Kelly, M.; Black, S.; Rowan, J.S. A calcrete-based U/Th chronology for landform evolution in the Sorbas basin, southeast Spain. *Quat. Sci. Rev.* **2000**, *19*, 995–1010. [CrossRef]

37. Candy, I.; Black, S.; Sellwood, B. U-series isochron dating of immature and mature calcretes as a basis for constructing Quaternary landform chronologies for the Sorbas basin, southeast Spain. *Quat. Res.* **2005**, *64*, 100–111. [CrossRef]

38. Ilott, S.H. Cosmogenic Dating of Fluvial Terraces in the Sorbas Basin, SE Spain. Ph.D. Thesis, University of Plymouth, Plymouth, UK, 2013.

39. García-Meléndez, E.; Goy, J.L.; Zazo, C. Neotectonics and Plio-Quaternary landscape development within the eastern Huércal-Overa Basin (Betic Cordilleras, Southeast Spain). *Geomorphology* **2003**, *50*, 111–133. [CrossRef]

40. Stokes, M. Plio-Pleistocene drainage development in an inverted sedimentary basin: Vera basin, Betic Cordillera, SE Spain. *Geomorphology* **2008**, *100*, 193–211. [CrossRef]

41. Farines, B.; Calvet, M.; Gunnell, Y. The summit erosion surfaces of the inner Betic Cordillera: Their value as tools for reconstructing the chronology of topographic growth in southern Spain. *Geomorphology* **2015**, *233*, 92–111. [CrossRef]

42. Centro Nacional de Información Geográfica. Available online: http://centrodedescargas.cnig.es (accessed on 14 June 2018).

43. Boulton, S.J.; Stokes, M. Which DEM is best for analyzing fluvial landscape development in mountainous terrains? *Geomorphology* **2018**, *310*, 168–187. [CrossRef]

44. ESRI. How To: Identify Ridgelines from a DEM. Available online: https://support.esri.com/en/technical-article/000011289 (accessed on 14 June 2018).

45. Alexander, R.W.; Calvo-Cases, A.; Arnau-Rosalén, E.; Mather, A.E.; Lázaro-Suau, R. Erosion and stabilisation sequences in relation to base level changes in the El Cautivo badlands, SE Spain. *Geomorphology* **2008**, *100*, 83–90. [CrossRef]

46. Della Seta, M.; Del Monte, M.; Fredi, P.; Miccadei, E.; Nesci, O.; Pambianchi, G.; Piacentini, T.; Troiani, F. Morphotectonic evolution of the Adriatic piedmont of the Apennines: An advancement in the knowledge of the Marche-Abruzzo border area. *Geomorphology* **2008**, *102*, 119–129. [CrossRef]

47. Pérez-Peña, J.V.; Azañón, J.M.; Azor, A.; Tuccimei, P.; Della Seta, M.; Soligo, M. Quaternary landscape evolution and erosion rates for an intramontane Neogene basin (Guadix–Baza basin, SE Spain). *Geomorphology* **2009**, *106*, 206–218. [CrossRef]

48. Antón, L.; Muñoz-Martín, A.; De Vicente, G. Quantifying the erosional impact of a continental-scale drainage capture in the Duero Basin, northwest Iberia. *Quat. Res.* **2018**, 1–15. [CrossRef]

49. Geach, M.R.; Stokes, M.; Telfer, M.W.; Mather, A.E.; Fyfe, R.M.; Lewin, S. The application of geospatial interpolation methods in the reconstruction of Quaternary landform records. *Geomorphology* **2014**, *216*, 234–246. [CrossRef]

50. Rodés, Á.; Pallàs, R.; Ortuño, M.; García-Meléndez, E.; Masana, E. Combining surface exposure dating and burial dating from paired cosmogenic depth profiles. Example of El Límite alluvial fan in Huércal-Overa basin (SE Iberia). *Quat. Geochronol.* **2014**, *19*, 127–134. [CrossRef]

51. Hancock, G.S.; Anderson, R.S.; Chadwick, O.A.; Finkel, R.C. Dating fluvial terraces with 10Be and 26Al profiles: Application to the Wind River, Wyoming. *Geomorphology* **1999**, *27*, 41–60. [CrossRef]

52. Braucher, R.; Merchel, S.; Borgomano, J.; Bourlès, D. Production of cosmogenic radionuclides at great depth: A multi element approach. *Earth Planet. Sci. Lett.* **2011**, *309*, 1–9. [CrossRef]

53. Granger, D.E.; Smith, A.L. Dating buried sediments using radioactive decay and muogenic production of ^{26}Al and ^{10}Be. *Nucl. Instrum. Methods Phys. Res. Sect. B* **2000**, *172*, 822–826. [CrossRef]

54. Granger, D.E.; Muzikar, P.F. Dating sediment burial with in situ-produced cosmogenic nuclides: Theory, techniques, and limitations. *Earth Planet. Sci. Lett.* **2001**, *188*, 269–281. [CrossRef]

55. Balco, G.; Rovey, C.W. An isochron method for cosmogenic-nuclide dating of buried soils and sediments. *Am. J. Sci.* **2008**, *308*, 1083–1114. [CrossRef]

56. Balco, G.; Stone, J.O.H.; Lifton, N.; Dunai, T. A complete and easily accessible means of calculating surface exposure ages or erosion rates from Be and Al measurements. *Quat. Geochronol.* **2008**, *3*, 174–195. [CrossRef]

57. Lal, D. Cosmic ray labelling of erosion surfaces: In situ nuclide production rates and erosion models. *Earth Planet. Sci. Lett.* **1991**, *104*, 424–439. [CrossRef]

58. CRONUS Calculator 2.3. Available online: https://hess.ess.washington.edu/ (accessed on 4 June 2018).

59. Mather, A.E.; Harvey, A.M.; Stokes, M. Quantifying long-term catchment changes of alluvial fan systems. *Geol. Soc. Am. Bull.* **2000**, *112*, 1825–1833. [CrossRef]

60. Mather, A.E.; Westhead, K. Plio/Quaternary strain of the Sorbas Basin, SE Spain: Evidence from soft sediment deformation structures. *Quat. Proc.* **1993**, *3*, 57–65.

61. Nash, D.J.; Smith, R.F. Multiple calcrete profiles in the Tabernas Basin, southeast Spain: Their origins and geomorphic implications. *Earth Surf. Process. Landf.* **1998**, *23*, 1009–1029. [CrossRef]

62. King, L. The pediment landform: Some current problems. *Geol. Mag.* **1949**, *86*, 245–250. [CrossRef]

63. Dumas, B. Glacis et croutes calcaires dans le Levant espagnol. *Bull. Assoc. Géogr. Fr.* **1969**, *46*, 553–561. [CrossRef]

64. Strudley, M.W.; Murray, A.B. Sensitivity analysis of pediment development through numerical simulation and selected geospatial query. *Geomorphology* **2007**, *88*, 329–351. [CrossRef]

65. Hodge, E.J.; Richards, D.A.; Smart, P.L.; Andreo, B.; Hoffmann, D.L.; Mattey, D.P.; González-Ramón, A. Effective precipitation in southern Spain (~266 to 46 ka) based on a speleothem stable carbon isotope record. *Quat. Res.* **2008**, *69*, 447–457. [CrossRef]

66. Carrión, J.S.; Fernández, S.; Jiménez-Moreno, G.; Fauquette, S.; Gil-Romera, G.; González-Sampériz, P.; Finlayson, C. The historical origins of aridity and vegetation degradation in southeastern Spain. *J. Arid Environ.* **2010**, *74*, 731–736. [CrossRef]

67. Martrat, B.; Jimenez-Amat, P.; Zahn, R.; Grimalt, J.O. Similarities and dissimilarities between the last two deglaciations and interglaciations in the North Atlantic region. *Quat. Sci. Rev.* **2014**, *99*, 122–134. [CrossRef]
68. Pla-Pueyo, S.; Viseras, C.; Soria, J.M.; Tent-Manclús, J.E.; Arribas, A. A stratigraphic framework for the Pliocene–Pleistocene continental sediments of the Guadix Basin (Betic Cordillera, S. Spain). *Quat. Int.* **2011**, *243*, 16–32. [CrossRef]
69. Braga, J.C.; Martín, J.M.; Quesada, C. Patterns and average rates of late Neogene-Recent uplift of the Betic Cordillera, SE Spain. *Geomorphology* **2003**, *50*, 3–26. [CrossRef]
70. Stokes, M.; Mather, A.E.; Belfoul, A.; Farik, F. Active and passive tectonic controls for transverse drainage and river gorge development in a collisional mountain belt (Dades Gorges, High Atlas Mountains, Morocco). *Geomorphology* **2008**, *102*, 2–20. [CrossRef]
71. Harvey, A.M.; Silva, P.; Mather, A.E.; Goy, J.; Stokes, M.; Zazo, C. The impact of Quaternary sea level and climatic change on coastal alluvial fans in the Cabo de Gata ranges, southeast Spain. *Geomorphology* **1999**, *28*, 1–22. [CrossRef]
72. Pastor, A.; Babault, J.; Teixell, A.; Arboleya, M.L. Intrinsic stream-capture control of stepped fan pediments in the High Atlas piedmont of Ouarzazate (Morocco). *Geomorphology* **2012**, *173*, 88–103. [CrossRef]
73. Völk, H.R. *Quartare Reliefentwicklung in Sudost-Spanien*; Heidelberger Geographische Arbeiten: Heidelberger, Germany, 1979; 143p.
74. Stokes, M. Plio-Pleistocene Drainage Evolution of the Vera Basin, SE Spain. Ph.D. Thesis, University of Plymouth, Plymouth, UK, 1997.
75. Stokes, M.; Mather, A.E. Response of Plio-Pleistocene alluvial systems to tectonically induced base-level changes, Vera Basin, SE Spain. *J. Geol. Soc.* **2000**, *157*, 303–316. [CrossRef]
76. Wenzens, G. Mittelquartäre klimaverhältnisse und reliefentwicklung im semiariden becken von Vera (Südostspanien). *Eiszeitalt. Ggw.* **1992**, *42*, 121–133.
77. Wenzens, G. The influence of tectonics and climate on the Villafranchian morphogenesis in semiarid Southeastern Spain. *Z. Geomorphol.* **1992**, *84*, 173–184.
78. Wenzens, G. Die Quartäre küstenentwicklung im mündungsbereich der flüsse Aguas, Antas und Almanzora in Südostspanien. *Erdundliches Wissen* **1991**, *105*, 131–150.
79. Meikle, C.; Stokes, M.; Maddy, D. Field mapping and GIS visualisation of Quaternary river terrace landforms: An example from the Rio Almanzora, SE Spain. *J. Maps* **2010**, *6*, 531–542. [CrossRef]
80. Silva, P.G.; Roquero, E.; López-Recio, M.; Huerta, P.; Martínez-Graña, A.M. Chronology of fluvial terrace sequences for large Atlantic rivers in the Iberian Peninsula (Upper Tagus and Duero drainage basins, Central Spain). *Quat. Sci. Rev.* **2017**, *166*, 188–203. [CrossRef]
81. Santisteban, J.I.; Schulte, L. Fluvial networks of the Iberian Peninsula: A chronological framework. *Quat. Sci. Rev.* **2007**, *26*, 2738–2757. [CrossRef]
82. Antón, L.; De Vicente, G.; Muñoz-Martín, A.; Stokes, M. Using river long profiles and geomorphic indices to evaluate the geomorphological signature of continental scale drainage capture, Duero basin (NW Iberia). *Geomorphology* **2014**, *206*, 250–261. [CrossRef]
83. Gibbard, P.L.; Lewin, J. River incision and terrace formation in the Late Cenozoic of Europe. *Tectonophysics* **2009**, *474*, 41–55. [CrossRef]
84. Bellin, N.; Vanacker, V.; Kubik, P.W. Denudation rates and tectonic geomorphology of the Spanish Betic Cordillera. *Earth Planet. Sci. Lett.* **2014**, *390*, 19–30. [CrossRef]